Vertical diffuse attenuation coefficient (K_d) based optical classification of IRS-P3 MOS-B satellite ocean colour data

R K Sarangi, Prakash Chauhan and S R Nayak

Marine and Water Resources Group, Remote Sensing Applications Area, Space Applications Centre (ISRO), Ahmedabad, India.

The optical classification of the different water types provides vital input for studies related to primary productivity, water clarity and determination of euphotic depth. Image data of the IRS-P3 MOS-B, for Path 90 of 27th February, 1998 was used for deriving vertical diffuse attenuation coefficient (K_d) and an optical classification based on K_d values was performed. An atmospheric correction scheme was used for retrieving water leaving radiances in blue and green channels of 412, 443, 490 and 550 nm. The upwelling radiances from 443 nm and 550 nm spectral channels were used for computation of vertical diffuse attenuation coefficient K_d at 490 nm. The waters off the Gujarat coast were classified into different water types based on Jerlov classification scheme. The oceanic water type IA (K_d range 0.035– 0.040 m^{-1}), type IB (0.042–0.065 m^{-1}), type II (0.07–0.1 m^{-1}) and type III (0.115–0.14 m^{-1}) were identified. For the coastal waters along Gujarat coast and Gulf of Kachchh, $K_d(490)$ values ranged between 0.15 m^{-1} and 0.35 m^{-1}. The depth of 1% of surface light for water type IA, IB, II and III corresponds to 88, 68, 58 and 34 meters respectively. Classification of oceanic and coastal waters based on K_d is useful in understanding the light transmission characteristics for sub-marine navigation and under-water imaging.

1. Introduction

Remote sensing reflectance is important for characterising the coastal and oceanic optical environment. The oceanic and coastal processes alter the optical properties of waters and these effects get manifested in the colour of the water. Remote sensing provides an extremely valuable tool for rapidly assessing the spatial variability of coastal and oceanic water reflectance patterns. Satellite based ocean colour sensors have been used to map biological and optical properties of the ocean on local and global scales. Data from Coastal Zone Colour Scanner (CZCS), which operated from 1978 to 1986, have been used in numerous studies to describe patterns of chlorophyll concentration, primary production and diffuse attenuation coefficient (Austin 1981; Sathyendranath *et al* 2000). The Indian IRS-P3 satellite carrying onboard three remote sensing payloads modular opto-electronic scanner (MOS), Wide Field Sensor (WiFS) and X-ray astronomy payload was launched successfully by the Polar Satellite Launch Vehicle (PSLV) on March 21st, 1996 from Sriharikota, India. The MOS payload comprises MOS-A, MOS-B & MOS-C modules. The module MOS-B comprises thirteen narrow channels ranging from 400 to 1010 nm and has a swath of 200 km and a relatively high radiometric resolution of 16 bit with 10 nm spectral band-width. The details of IRS-P3 MOS-B technical characteristics are available in Mohan *et al* (1997). The MOS-B module of the MOS payload has been designed to study ocean-atmospheric system and in particular ocean colour related studies.

Light availability is a critical regulator of oceanic and coastal production of phytoplankton (Tyler 1975; Pennock and Sharp 1986). As a result basic research efforts require information on the availability of light in oceanic and coastal waters. The measurement of diffuse attenuation

Keywords. Diffuse attenuation coefficient; optical classification; IRS-P3 MOS-B data.

Proc. Indian Acad. Sci. (Earth Planet. Sci.), **111**, No. 3, September 2002, pp. 237–245

coefficient (K_d) is of particular interest for this purpose, which defines the presence of light versus depth, the depth of euphotic zone, and ultimately the maximum depth of primary production. Smith and Baker (1978) have classified ocean water by relating the diffuse attenuation coefficient to the plant pigment content. The term diffuse attenuation coefficient, most commonly used for the downwelling plane irradiance, $K_d(z;\dot{\lambda})$, varies systematically with wavelength over a wide range of waters from very clear to very turbid. Jerlov (1976) exploited this behaviour of K_d to develop a frequently used classification scheme for oceanic waters based on the spectral shape of K_d. The diffuse attenuation coefficient is also an indicator of water clarity and water quality and it is of interest to those requiring a prediction of light propagation qualities of water for passive or active optical systems for imaging, e.g., underwater photography or video camera systems, sub-marine navigation and optical bathymetry.

Keeping the above discussion in mind the present study has been taken up for

- pre-processing of IRS-P3 MOS-B data,
- implementation of an atmospheric correction methodology on the multi-spectral channels, and
- implementation of a diffuse attenuation coefficient (K_d) algorithm for generation of K_d map for water type classification.

2. Study area

IRS-P3 MOS-B image data of the Path 90 for 27th February 1998 was used in the present study. Different locations along the coastal waters of Gujarat and oceanic waters were selected to understand the spectral behaviour of MOS radiances at the top of the atmosphere and water leaving radiances. Stations were selected within the image as **(1)** near the Gulf of Kachchh mouth, **(2)** in the coastal water and **(3)** in the deep oceanic waters (figure 1).

Figure 1. Different water types shown on IRS-MOS image data, off Gujarat coast. The geographic co-ordinates of the image comprises, longitude: 67.45–70.72°E and latitude: 17.82–23.78°N.

3. Methodology

3.1 *Pre-processing of the IRS-P3 MOS-B data*

IRS-P3 MOS-B image data were extracted into thirteen channel BSQ file format from level-0 data set supplied to users. The Digital Number (DN) values for each of the channels were converted into top of the atmospheric (TOA) radiance by applying gain factor for each spectral channel, supplied along with the level-0 data set. Radiance images generated through this process were used for subsequent processing. TOA radiance values at selected stations were plotted against wavelength, to generate spectral curves for different water types (figure 2).

3.2 *Atmospheric correction of IRS-P3 MOS-B data*

In the case of oceanic remote sensing, the total signal received at the satellite altitude is dominated by radiance contributed through atmospheric scattering processes and only 8–10% of the signal corresponds to oceanic reflectance. Therefore it is mandatory to correct for atmospheric effect to retrieve any quantitative parameter from space. The radiance received by a sensor at the top of the atmosphere (TOA) in a spectral band centred at a

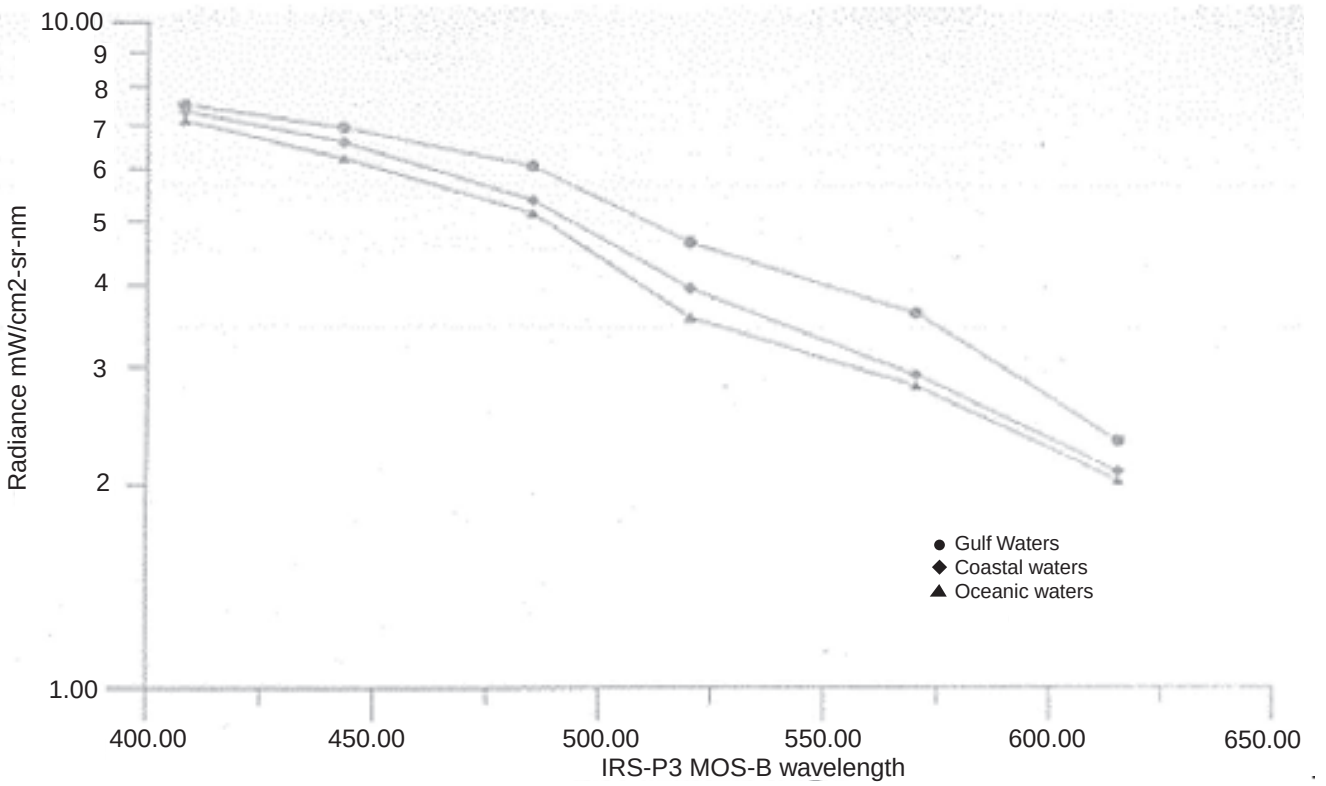

Figure 2. Top of the atmospheric (TOA) radiances derived from IRS-P3 MOS-B data over different water types.

wavelength $\lambda_i, L_t(\lambda_l)$ can be divided into the following components

$$L_t(\lambda_i) = L_a(\lambda_i) + L_r(\lambda_i) + T(\lambda_i)L_g(\lambda_i) + t(\lambda_i)L_w(\lambda_i) \quad (1)$$

where, L_a and L_r are the radiances generated along the optical path by scattering in the atmosphere due to aerosol and Rayleigh scattering. L_g is the specular reflection or sun glitter component and L_w is the desired water leaving radiance. In this equation, T and t are the direct and diffuse transmittance of the atmosphere, respectively. Gordon and Clarke (1981) have shown that for NIR channels the water leaving radiance coming out of the ocean can be approximately put equal to zero and by neglecting the effect of sun glitter equation (1) can be written as

$$L_t(\lambda_i) = L_a(\lambda_i) + L_r(\lambda_i) \text{ for } \lambda > 750\,\text{nm} L_w \sim 0. \quad (2)$$

From equation (2) it is clear that for MOS-B channels 765 nm and 865 nm the TOA radiance corresponds to the contribution coming from the atmosphere alone, since water leaving radiance $L_w(765\ \&\ 865)$ has been assumed to be equal to zero. The Rayleigh scattering term $L_r(\lambda_l)$ can be computed using well-established formulation.

$$L_r(\lambda_i) = F_0 w_0 \tau_r P_r / 4\pi \cos\theta \quad (3)$$

where, F_0 is extraterrestrial solar flux at the top of the atmosphere, w_0 is single scattering albedo equal to 1, τ_r is Rayleigh optical thickness, P_r is Rayleigh scattering phase function and θ is solar zenith angle. Using equation (3) Rayleigh path radiances were calculated for 765 and 865 nm spectral bands of MOS-B data for a sub-scene of 200/200 pixels and then extended to the entire image. The aerosol path radiance $(L_a(\lambda))$ is then estimated as

$$L_a(\lambda_l) = L_t(\lambda_l) - L_r(\lambda_l) \quad \text{for } \lambda_i > 750\,\text{nm}. \quad (4)$$

Since MOS-B payload has two channels at 765 and 865 nm in the NIR region, a relationship is obtained for the spectral behaviour of the aerosol optical depth from these two bands. Gordon and Wang (1994) have proposed an exponential relationship for the spectral behaviour of aerosol

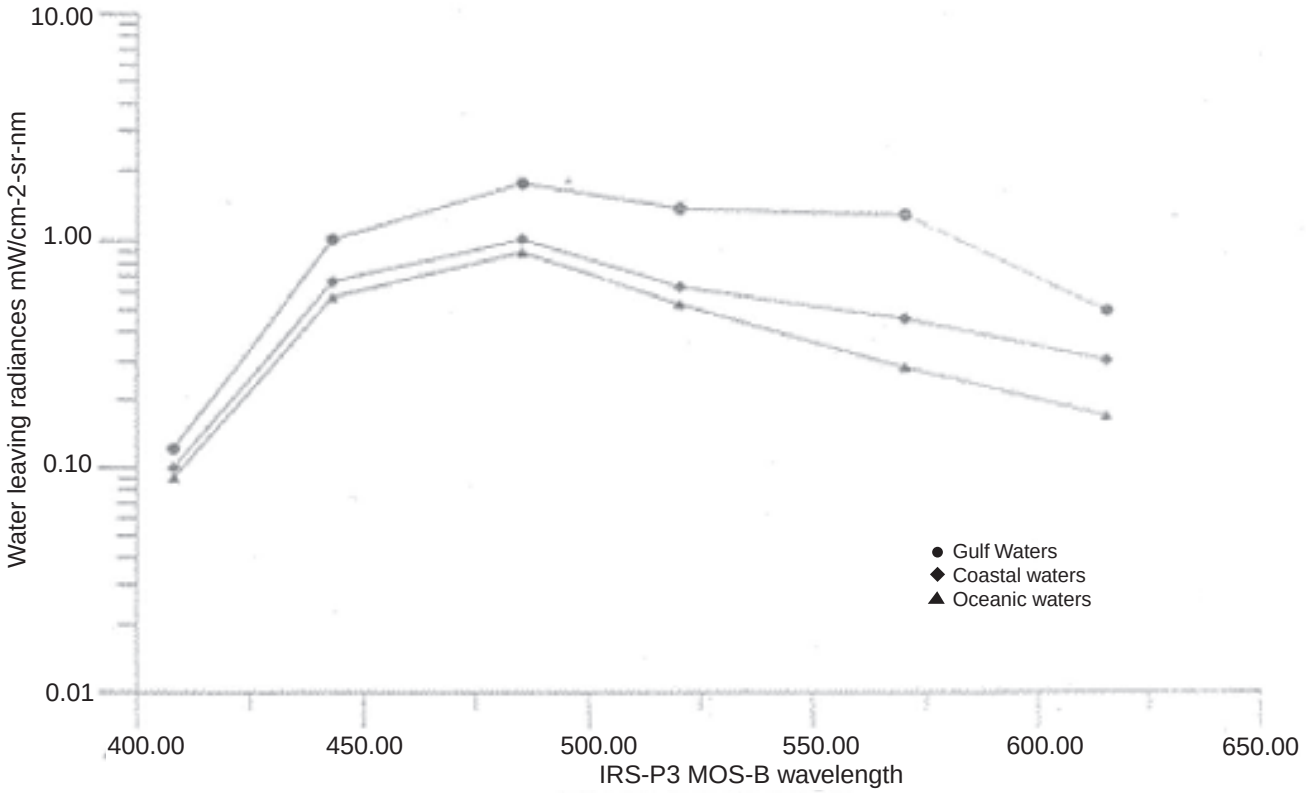

Figure 3. Water leaving radiances (mW cm^{-2}-sr-nm) derived from MOS-B data after atmospheric correction over different water types locations.

optical depth which has been used for the SeaWiFS atmospheric correction algorithm. A similar approach is used here and an Angstrom exponent based on an exponential relation was calculated using 765 and 865 nm spectral data for each pixel. The aerosol optical thickness is extrapolated to visible channels using this exponential relation, which is represented as

$$\epsilon(c) = L_a(765)/L_a(865), \tag{5}$$

$$L_w(\lambda_{l<750}) = \left[\frac{L_{\mathrm{ac}}(\lambda_i) - L_a(865)^* \exp[\log \epsilon/(865-765)]^*(865-\lambda)}{t(\lambda)} \right] \tag{6}$$

where $L_{ac}(\lambda_i)$ is the Rayleigh and ozone corrected radiances for $\lambda < 750$ nm and $t(\lambda)$ is the diffused transmittance term. Using equation (6) water leaving radiances images were generated for short wavelength channels e.g., 412, 443, 490, 520 and 550 nm spectral bands. Effectively, a mono-modal aerosol size distribution is implicitly assumed in this approach, however for bi-modal particle size distribution the accuracy of the algorithm may suffer. Figure 4 shows the atmospherically corrected images of 443 and 550 nm spectral channels. Figure 3 shows the water leaving spectral curves obtained for different water types.

3.3 *Diffuse attenuation coefficient* (K_d)

The vertical downwelling diffuse attenuation coefficient, K_d is an apparent optical property since its magnitude depends on the irradiance distribution at the time and point of measurement (Preisendorfer 1961). The diffuse attenuation coefficient K_d for any wavelength or spectral band is defined as

$$K_d = 1/E(z)^* \, \mathrm{d}E(z)/\mathrm{d}z \tag{7}$$

where E is the irradiance energy and z is the depth. The diffuse attenuation coefficient algorithm for determining the downwelling irradiance coefficient, or K, for case 1 waters used the upwelling radiance from the 443 nm and 550 nm bands. The algorithm for K_d at 490 nm has the following form (Austin and Petzold 1981).

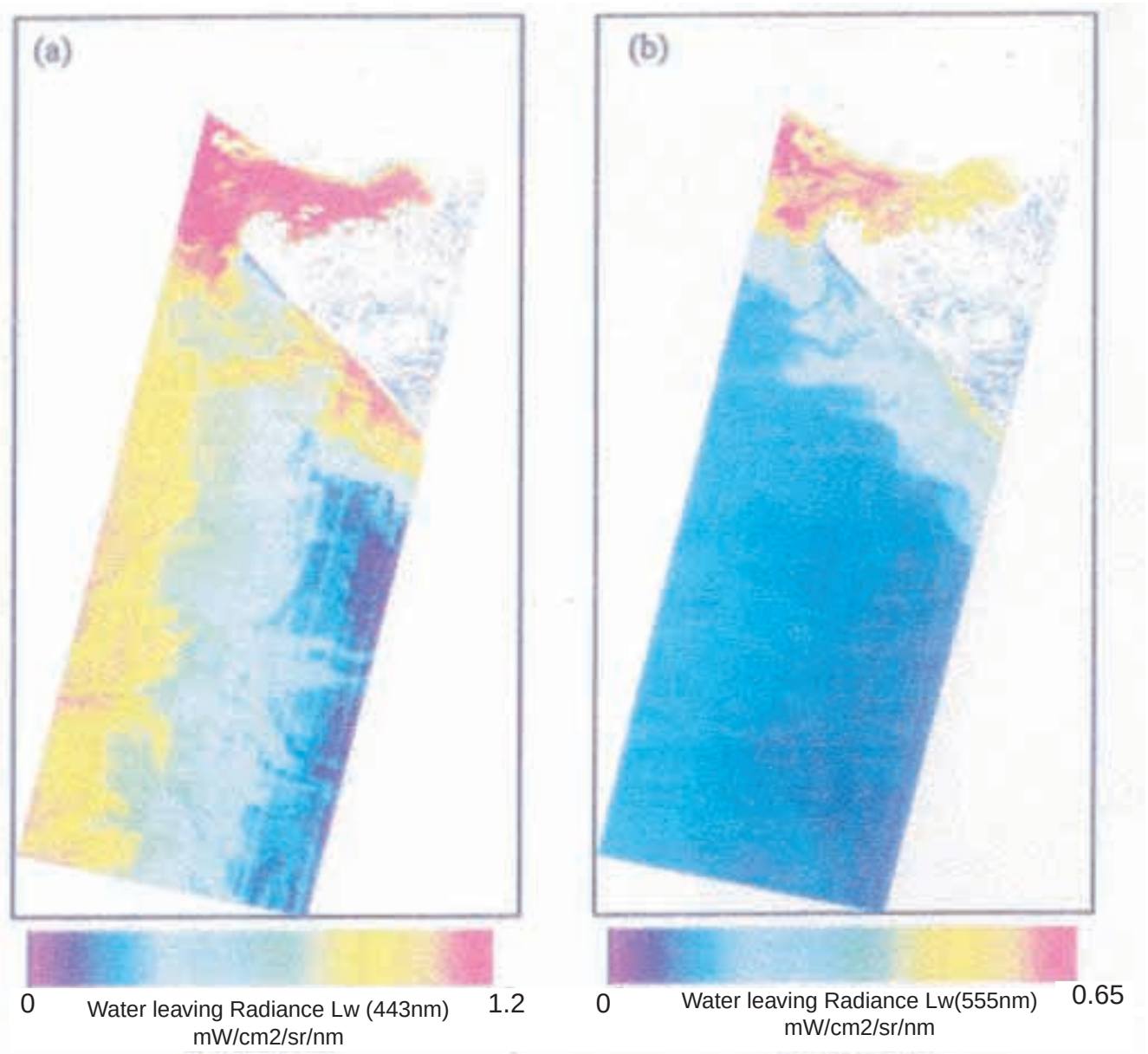

Figure 4. Water leaving radiance images of IRS-MOS data **(a)** 443 nm **(b)** 555 nm channels.

$$K_d(490) = 0.0883^{*}[L_w(443)/L_w(550)]^{-1.491} + 0.022 \quad (8)$$

where $L_w(443)$ and $L_w(550)$ are the upward water leaving radiances in the 443 and 550 nm channels, respectively. The atmospherically corrected 443 and 550 nm channel data were used for the calculation of the K_d map from MOS-B data. The algorithm was devised using *in situ* measurements from a variety of sources (Austin and Petzold 1981). Using a regression analysis of the data sets, equation (8) was obtained at a correlation coefficient value of $r^2 = 0.901$. The image generated using the MOS-B data for 27th February 1998 and classified according to Jerlov scheme is shown in figure 5.

4. Results and discussion

As mentioned earlier the analysis of the radiance image was done for wavelengths 408, 443, 485, 520, 570, 615 nm over three different stations at the Gulf of Kachchh mouth, in coastal waters and in deep water. It is clear that the radiance value of TOA varied at station locations. For the Gulf of Kachchh waters, the observed radiances are relatively higher (figure 2). This is due to high turbidity which results in low light absorption and greater backscattering due to the high concentrations of inorganic particulate matter. There may also be an increase in reflected radiances due to the shallow bottom. Near coastal waters of Saurastra region show lesser radiance values than

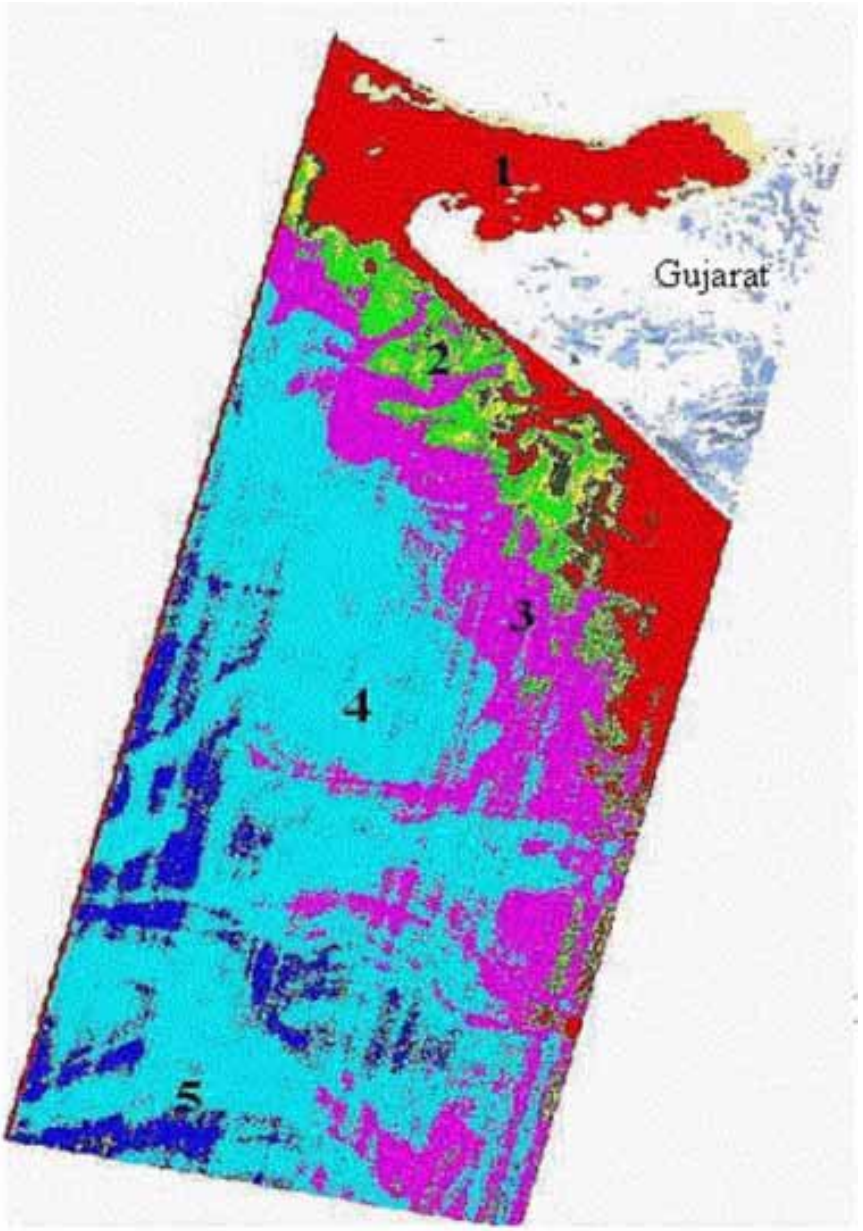

Figure 5. Vertical diffuse attenuation coefficient K_d (490 nm) from IRS-P3 MOS-B data for 27/02/97, Path 90 off Gujarat coast.

the Gulf waters, where the distribution of algal cells like phytoplankton and other pigments may cause the absorption of light in the blue-green. Since TOA radiance values are dominated by Rayleigh and aerosol path radiance it becomes difficult to infer the spectral properties of different types of waters from TOA radiance values. Analysis of the atmospherically corrected images show the water leaving radiance variability from turbid waters of Gulf of Kachchh to relatively clear oceanic waters. L_w values increase with wavelength from 408 to 520 nm and decrease for 570 and 615 nm. The water leaving radiance (L_w) is more for Gulf waters due to high turbidity and presence of yellow substance.

The K_d (490 nm) images generated in this study show four major classes of oceanic water type off Gujarat coast and a distinct boundary between oceanic and coastal waters. The lowest values as derived from the K_d image corresponds to a range between 0.03 and 0.05 m^{-1}, which corresponds to water type IA. The other K_d class values and corresponding water type as obtained from IRS-MOS data are shown in table 1. Since the K_d is also an indicator of water clarity, Jerlov (1976) has given estimates of depth of 1% of light availability for different water types. The information on light availability is very useful for euphotic depth estimation.

Further analysis has been carried out to compute K_d (490) for the *in situ* radiometer data being

Table 1. *Vertical diffuse attenuation coefficients K_d (490) as derived from IRS-P3 MOS-B data off Gujarat coast for classified areas 1–5 (figure 5).*

Sr. no.	K_d range (m^{-1})	Water type	1% light depth (m)
1	0.03 – 0.05	Oceanic water IA	88.3
2	0.05 – 0.07	Oceanic water IB	68.3
3	0.07 – 0.11	Oceanic water II	57.6
4	0.12 – 0.14	Oceanic water III	33.8
5	> 0.15	Coastal waters	–

Table 2. *Vertical diffuse attenuation coefficient K_d(490) derived from in situ LICOR-1800 underwater radiometer data collected during the IRS-P3 MOS-B validation cruises in between April 1996–October 1997 in the Arabian Sea.*

Station No.	Date	Latitude (°N)	Longitude (°E)	*In situ* K_d(490) (Preisonderfer's equation)	*In situ* K_d(490) (Austin & Petzolt's equation)
1	14.04.96	16°31.01′	78°28.04′	0.0388	0.0388
2	16.04.96	16°45.49′	69°50.08′	0.0521	0.0640
3	10.04.97	17°46.09′	69°24.11′	0.0362	0.0362
4	11.04.97	19°53.00′	69°43.05′	0.0585	0.0585
5	11.04.97	20°17.24′	69°51.42′	0.0607	0.0607
6	12.04.97	20°48.09′	69°56.59′	0.0791	0.0791
7	13.04.97	21°31.12′	69°31.43′	0.1338	0.1338
8	13.04.97	21°31.39′	69°33.58′	0.1745	0.1745
9	15.04.97	20°30.11′	70°53.07′	0.1132	0.1132
10	15.04.97	20°10.52′	70°46.31′	0.0828	0.0827
11	08.10.97	16°31.34′	73°06.40′	0.1396	0.1396
12	08.10.97	16°36.04′	73°15.06′	0.3479	0.3479
13	11.10.97	21°12.76′	69°50.58′	0.1892	0.1892
14	13.10.97	21°38.03′	69°33.24′	0.2565	0.2565
15	13.10.97	21°38.36′	69°34.68′	0.3663	0.3664
16	14.10.97	21°32.00′	69°35.40′	0.2003	0.2002

collected during 3 validation cruises in between April 1996 and October 1997 for IRS-P3 MOS-B sensor and are presented in table 2, which are also in good comparison with the attenuation range for Arabian Sea water. A near-synchronous satellite pass data (16.10.97) has been analyzed to relate with the attenuation coefficient (K_d) values obtained from the *in situ* computation (table 2) for four points, which is shown in figure 6. The K_d range does not vary much even if it does not correlate well, as there is a difference of 3–4 days with respect to satellite pass date.

Verkey and Kesavadas (1976) also reported a similar diffusive attenuation coefficients in the Arabian Sea with the values of K_d ($> .15$ to .46) in the coastal waters and < 0.15 in the offshore waters. The oceanic water shows the K_d values in the range of 0.03 to 0.15. Since the K_d algorithm used in this study works well only in oceanic waters, further sub-classification of coastal water types is not attempted in this study.

5. Conclusion

The IRS-P3 MOS-B data have shown the potential for the classification of different water types based on Jerlov's classification scheme. The waters off the Gujarat coast are classified as oceanic water type IA (K_d range 0.035–0.040 m^{-1}), type IB (0.042–0.065 m^{-1}), type II (0.07–0.1 m^{-1}) and type III (0.115–0.14 m^{-1}). For the coastal waters along Gujarat coast and Gulf of Kachchh, K_d(490) values ranged from 0.15 m^{-1} to 0.35 m^{-1}. The depth of 1% of surface light for water type IA, IB, II and III corresponds to 88.3, 68.3, 57.6 and 33.8 m respectively. A rough correspondence between chlorophyll concentration and Jerlov oceanic water types also is drawn. Water type IA corresponds to chlorophyll concentration close to 0.05 mg/m^3, water type IB corresponds to concentration close to 0.1 mg/m^3 and water type II have chlorophyll concentration close to 0.5 mg/m^3 and water type III corresponds to chlorophyll concentrations between 1.5 and 2.0 mg m^3. The K_d is also used as a measure of water quality and to predict the depth

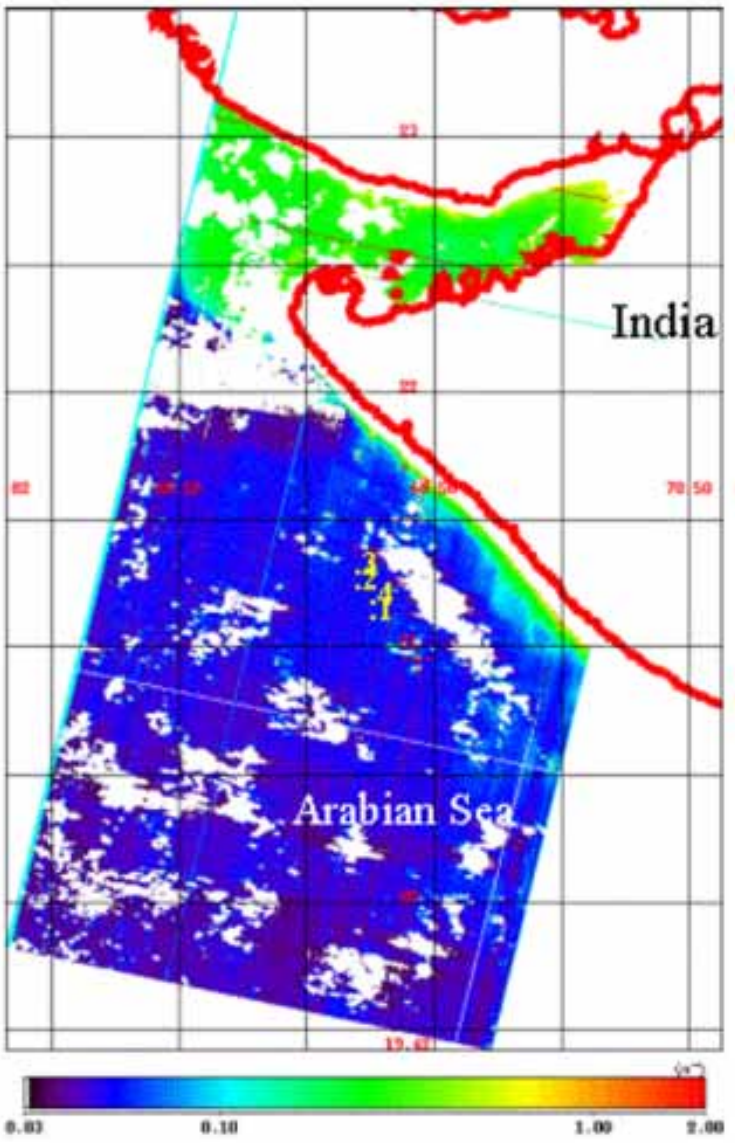

K_d Values for Stations 1 – 4

	MOS-B Data (16.10.97)	*In situ* Data (Table 2)
1.	0.092 m^{-1}	0.1892 m^{-1} (11.10.97)
2.	0.127 m^{-1}	0.2565 m^{-1} (13.10.97)
3.	0.181 m^{-1}	0.366 m^{-1} (13.10.97)
4.	0.106 m^{-1}	0.2002 m^{-1} (14.10.97)

Figure 6. IRS-P3 MOS-B derived diffuse attenuation coefficient, K_d (490) image showing *in situ* validated data points for near-synchronous satellite pass date.

of the euphotic zone. The information on water clarity can be used for generation of water clarity maps using MOS-B data and IRS-P4 Ocean Colour Monitor (OCM) data. Although the results obtained in this study on K_d values look quite good, a validation study with satellite synchronous passes is required to assess the accuracy of the algorithm used and results obtained. Further work is also needed for seasonal and long term monitoring of vertical diffuse attenuation in the Arabian Sea.

Acknowledgements

The authors are thankful to Dr. R R Navalgund, former Deputy Director, Remote Sensing Application Area and Director, Space Applications Center for providing necessary guidance and facilities for carrying out the work.

References

Austin R W and Petzold T J 1981 The determination of the diffuse attenuation coefficient of sea water using the Coastal Zone Colour Scanner, in Oceanography from Space, (ed) J F R Gower (New York: Plenum) 239–256

Austin R W 1981 Remote sensing of the diffuse attenuation coefficient of ocean water; In: Proc. of the 29th symposium of the AGARD electromagnetic wave propagation panel on special topics in optical propagation, (California, USA: Monterey)

Gordon H R and Clark 1981 Clear water radiance for atmospheric correction of CZCS imagery; *App. Optics* **20** 4157–4180

Gordon H R and Wang M 1994 Retrieval of water leaving radiance and aerosol optical thickness over the oceans with SeaWiFS: A preliminary algorithm; *App. Optics*, **33** 443–452

Jerlov N G 1976 *Optical Oceanography*, (New York: Elsevier) 118–122

Mohan M, Chauhan P, Raman M, Solanki H U, Mathur A K, Nayak S R, Jayaraman A, Satheesh S K and Krishnan S K 1997 Initial results of MOS validation experiment over the Arabian Sea, atmospheric correction aspects; In: Proceedings of the First International Workshop on MOS-IRS and ocean colour, DLR, Berlin, April 28–30, 1997

Pennock J R and Sharp J H 1986 Phytoplankton production in the Delaware estuary: Temporal and spatial variability; *Mar. Ecol. Prog. Ser.* **34** 143–155

Preisendorfer R W 1961 A generalised invariant imbedding relation: *Proc. Nat. Acad. Sci.* **47(4)** 591–594

Sathyendranath S, Bukata R P, Arnone R, Dowell M D, Davis C O, Babin M, Berthon J F, Kopelevich O V and Campbell J W 2000 Remote sensing of ocean colour in coastal, and other optically-complex waters: Reports of the international ocean-colour coordinating group, Report No. 3, 23–46

Smith R C and Baker K 1978 Optical classification of natural waters; *Limno. Oceanogr.* **23(2)** 260–267

Tyler J E 1975 The *in situ* quantum efficiency of natural phytoplankton populations; *Limno. Oceano.* **20** 976–980

Varkey M J and Kesavadas V 1976 Light transmission characteristics of the north Arabian Sea during December–May; *Indian J. Marine Sci.* **5** 147–151